A&A 425, 1069–1074 (2004)
DOI: 10.1051/0004-6361:20041185

Astronomy & Astrophysics

γ-ray emission from microquasars: A numerical model for LSI +61°303

V. Bosch-Ramon and J. M. Paredes

Departament d'Astronomia i Meteorologia, Universitat de Barcelona, Av. Diagonal 647, 08028 Barcelona, Spain
e-mail: vbosch@am.ub.es; jmparedes@ub.edu

Received 29 April 2004 / Accepted 24 June 2004

Abstract. We explore the possible association between the microquasar LSI +61°303 and the EGRET source 2CG 135+01/3EG J0241+6103 by studying, with a detailed numerical model, whether this system can produce the emission and the variability detected by EGRET (>100 MeV) through inverse Compton (IC) scattering. Our numerical approach considers a population of relativistic electrons entrained in a cylindrical inhomogeneous jet, interacting with both the radiation and the magnetic fields, taking into account the Thomson and Klein-Nishina regimes of interaction. Our results reproduce the observed spectral characteristics and variability at γ-rays, thus strengthening the identification of LSI +61°303 as a high-energy γ-ray source.

Key words. X-rays: binaries – stars: individual: LSI +61°303 – gamma-rays: observations – gamma-rays: theory

1. Introduction

LSI +61°303 is a High Mass X-ray binary system whose optical counterpart is a bright ($V \sim 10.8$) star of B0 V spectral type (Paredes & Figueras 1986). In fact, the companion star is a Be, and the compact object could be likely a neutron star (Hutchings & Crampton 1981). Taylor et al. (1980) found that LSI +61°303 presented strong radio outbursts each 26.5 days, which was associated to the orbital period of the binary system (Taylor & Gregory 1982). A four-year modulation of the maximum flux during radio outbursts (Paredes 1987; Gregory et al. 1989) was associated either to a precession of a possible jet or to variations in the accretion rate (Gregory et al. 1989). Optical observations carried out by Paredes & Figueras (1986) detected variable emission at timescales similar to the radio ones and, from ROSAT data, Goldoni & Mereghetti (1995) found also X-ray variability on a timescale of days. The microquasar nature of LSI +61°303 was established when a relativistic jet structure was detected through VLBI observations of this source (Massi et al. 2001).

LSI +61°303 was proposed by Gregory & Taylor (1978) as the possible counterpart of the high-energy γ-ray source 2CG 135+01 (Hermsen et al. 1977; Swanenburg et al. 1981), which was also detected by EGRET[1] (3EG J0241+6103) (Kniffen et al. 1997; Hartman et al. 1999). The proposed association between LSI +61°303 and the high-energy γ-ray source is still unclear due to the high uncertainty in position of EGRET sources. Nevertheless, no radio loud active galactic nucleus or strong radio pulsar is known within the error box of 3EG J0241+6103, which includes LSI +61°303 (Kniffen et al. 1997). Variability studies can help us to reinforce the association between LSI +61°303 and 3EG J0241+6103. Tavani et al. (1998) found that the γ-ray flux varied by a factor of 3. Also, Wallace et al. (2000) showed that in the EGRET viewing period 211.0 (1993 February 25–March 9) there was a γ-ray flare at an orbital phase around 0.5. Moreover, Massi (2004) presented a variability analysis of the EGRET data, obtaining a γ-ray period of 27.4 ± 7.2 days, in agreement with the orbital one. The results of that work also seem to suggest the presence of two peaks in the γ-ray flux: the first one would be in a phase around 0.2 (periastron passage, Casares et al. 2004), which was not covered in the data studied by Wallace et al. (2000), and the second one would be in a phase around 0.5 (like in the work of Wallace et al. 2000). It is worth mentioning that X-ray observations performed by ROSAT just six months before the EGRET viewing period 211.0 (1992 August–September) showed also an X-ray peak at an orbital phase around 0.5 (Peracaula 1997; Taylor et al. 1996). All these results strengthen the 3EG J0241+6103/LSI +61°303 association. At very high-energy γ-rays, Hall et al. (2003) gave upper limits for the emission associated to this source from observations performed with the Cherenkov telescope Whipple.

Several models have been proposed in order to explain the high energy emission of this source (e.g. Taylor et al. 1996; Punsly 1999; Harrison et al. 2000; Apparao 2001; Leahy 2001, 2004). Two typical scenarios have been proposed: a Be star plus a non-accreting pulsar or an accreting compact object with the same stellar companion. The most of the models mentioned above focused on the IC scattering of stellar photons by relativistic electrons as the mechanism for generating X-rays and/or γ-rays. The work of Punsly (1999) deserves a particular mention, since Synchrotron Self Compton (SSC)

[1] http://cossc.gsfc.nasa.gov/egret

scattering plays an important role therein, like in the present paper. We are interested in investigating whether LSI +61°303 is able to generate the high-energy γ-ray emission detected by EGRET. However, in the present work, we have performed accurate numerical calculations, taking into account the electron energy losses, to obtain the spectral emission from external Compton (EC) and SSC interactions in the Thomson and Klein-Nishina regimes. Moreover, unlike the pulsar wind shock model (first proposed by Maraschi & Treves 1981 and adopted also by, e.g., Harrison et al. 2000; Leahy 2004), we suppose that the electrons are entrained within a jet, which is ejected from the compact object. As a matter of fact, the discovering of relativistic radio jets, very similar to those observed in other microquasars (Mirabel & Rodríguez 1999), gives strong support to the accreting compact object scenario. It should be noted that leptonic jet models are not the only way to explain emission at EGRET energies. For instance, in the context of a high-mass microquasar like LSI +61°303, a hadronic jet model emitting γ-rays through pion-decay (see, i.e., Romero et al. 2003) could also be applied. In such a case, neutrinos would be expected also, as well as an EGRET spectrum harder than the one produced in the leptonic case, due to the much lower rate of losses for protons than for electrons in the jet.

LS 5039 (3EG J1824+1514) (Paredes et al. 2000a; Ribó 2002) is another microquasar and EGRET source candidate, sharing similar characteristics with LSI +61°303: both sources are high mass X-ray binaries, both sources seem to harbor a neutron star (for LS 5039, McSwain et al. 2004), both present persistent radio jets (for LS 5039, Ribó 2002; for LSI +61°303, see Massi et al. 2001 and 2004), the apparent absence of inner disk features in the X-ray spectrum, their moderate levels of radio and X-ray emission (for LSI +61°303, in the quiescent state), their possible nature as high-energy γ-ray emitters, and that both of them are likely fed by wind from the primary (for LSI +61°303, unless perhaps around periastron). Our model, previously applied to LS 5039 (Bosch-Ramon & Paredes 2004), has in LSI +61°303 a new interesting object of application.

This paper is organized as follows: in Sect. 2 we explain briefly our model, the application of the model to LSI +61°303 and its results are presented in Sect. 3, and the discussion of these results is developed in Sect. 4.

2. The model

In this model, we assume that the leptons in the jet dominate the radiative processes related to the γ-ray production. The relativistic population of electrons, already accelerated and flowing away into the jet, is exposed to external photons as well as to the synchrotron photons emitted by the electrons, since we take into account the magnetic field in our model. The γ-ray emitting region, the γ-jet, is assumed to be closer to the compact object than the observed radio jets. This γ-jet is supposed to be short enough to be considered cylindrical. The magnetic field (B_γ) has been taken to be constant, as an average along the jet. We have included the interaction between the relativistic electrons and both the magnetic and the radiation fields. The energy losses of the relativistic leptonic plasma within the γ-jet are mainly due to synchrotron emission, SSC scattering, and EC scattering. Due to the importance of the losses, the electron energy distribution density along the γ-jet model varies significantly, and in this sense the γ-jet is non-homogeneous. The γ-jet is studied by splitting it into cylindrical transverse cuts or slices. The size of the slices has to be suitable in order to get almost homogeneous physical conditions within each one (energy densities of the radiation and the electrons). Regarding IC interaction, we have used the cross-section of Blumenthal & Gould (1970): $\sigma(x, \epsilon_0, \gamma_e)$, which takes into account the low- and the high-energy regimes of interaction (i.e. the Thomson and Klein-Nishina regimes), ϵ_0 is the seed photon energy, γ_e is the scattering electron Lorentz factor, and x is actually a function which depends on both of the former quantities and on the scattered photon energy (ϵ).

The electron distribution is assumed to be initially a power law ($N(\gamma_e) \propto \gamma_e^{-p}$, where γ_e is the electron Lorentz factor), which evolves under the conditions imposed by the magnetic and the radiation fields. Thus, the electron distribution function of a certain slice ($N(\gamma_e, z)$) depends on both the distance to the compact object (z) and γ_e. The components of the total seed photon radiation field ($U(\epsilon_0, z)$) are any present external radiation field ($U_{ext}(\epsilon_0, z)$) and the synchrotron radiation field produced by the relativistic electrons within the jet, all of them in the reference frame of the jet (for the external photon fields, see Dermer & Schlickeiser 2002).

The free parameters of the model are B_γ and the maximum electron Lorentz factor at the slice closest to the compact object (γ_{e0}^{max}). The leptonic kinetic luminosity or leptonic jet power (L_{ke}) is set free also, and it is scaled with the observed luminosity, in order to reproduce the observations.

The luminosity per energy unit in the jet's reference frame (L_ϵ) is presented in Eq. (1). The photon flux per energy unit or spectral photon distribution[2] in the reference frame of the observer ($I'_{\epsilon'}$) is shown in Eq. (2). The magnitudes with ($'$) are in the observer reference frame.

$$L_\epsilon = \epsilon \sum_{z_{min}}^{z_{max}} V_{slice}(z) \int_{\epsilon_0^{min}(z)}^{\epsilon_0^{max}(z)} \int_{\gamma_e^{min}(z)}^{\gamma_e^{max}(z)} \frac{U(\epsilon_0, z)}{\epsilon_0} \times N(\gamma_e, z) \frac{d\sigma(x, \epsilon_0, \gamma_e)}{d\epsilon} d\gamma d\epsilon_0 \quad (1)$$

$$I'_{\epsilon'} = \frac{\delta^{2+p}}{4\pi D^2 \epsilon'} L_{\epsilon'} \quad (2)$$

where δ is the Doppler factor of the jet, D is the distance from LSI +61°303 to the observer, and $V_{slice}(z)$ is the volume of the slice at a distance z from the compact object. For further details of the model, see Bosch-Ramon & Paredes (2004).

3. Application of the model to LSI +61°303

In this section, we explore the possible nature of LSI +61°303 as a high-energy γ-ray emitter. We apply our model going

[2] In our previous paper (Bosch-Ramon & Paredes 2004), the factor ϵ_0 in the denominator of the integrand in Eq. (1) was inadvertently left out (see Eq. (12) in that work), although correctly included in the calculations. Also, the notation related to calculation reference frame has been clarified.

Table 1. Parameter values.

Parameter	Description	Derived values from observations
$\Gamma_{\rm jet}$	jet Lorentz factor	1.25
θ	angle between the jet and the observer line of sight	30°
$v_{\rm jet}$	jet velocity	$0.6c$
a	orbital semi-major axis	5×10^{12} cm
e	orbital eccentricity	0.7
D	distance to the observer	2 kpc
$L_{\rm star}$	star total luminosity	2×10^{38} erg s^{-1}
$I_{>100\ \rm MeV}$	photon flux at the EGRET band	8×10^{-7} photon cm^{-2} s^{-1}
Γ	photon index at the EGRET band	2.2
Parameter	**Description**	**Adopted values**
R_γ	γ-jet radius	10^7 cm
$L_{\rm ac}$	accretion disk luminosity	$10^{-9}\ M_\odot\ c^2$ yr^{-1}

through different magnetic field strengths and maximum electron Lorentz factors in order to estimate the best parameter values to reproduce the EGRET data. Afterwards, we study the implications of the orbital eccentricity on the stellar photon density and the accretion rate, and how it yields variability at high-energy γ-rays. We note that in this work we have assumed that the external photon field is solely due to the stellar radiation field ($U_{\rm star}(\epsilon_0, z)$), taken to be a black-body. We have not considered other possible sources of external photons like a disk or a corona. For a semi-analytical model of an inhomogeneous jet accounting for all the external photon fields, see Bosch-Ramon et al. (2004).

3.1. Parameter election for LSI +61°303

LSI +61°303 is an X-ray binary system located at an estimated distance of 2 kpc (Frail & Hjellming 1991). The bolometric luminosity of the companion star has been taken to be $L_{\rm star} \sim 2 \times 10^{38}$ erg s^{-1}. The more accurate value for the radio period, $P = 26.4960 \pm 0.0028$ days, assumed to be equal to the orbital period, was determined by Gregory (2002), and the eccentricity is taken in concordance with Martí & Paredes (1995) and Casares et al. (2004): $e \sim 0.7$. The orbital semi-major axis will be adopted as it is usual in the literature: $a = 5 \times 10^{12}$ cm. We define the distance between the companion star and the compact object as $R_{\rm orb}$. From MERLIN observations carried out by Massi et al. (2004), the jet velocity ($v_{\rm jet}$) is taken to be $0.6c$. As it is stated in that paper, the jet could be precessing, implying a possibly strong variation of θ. A typical value for θ of $\pi/6$ has been adopted. This $v_{\rm jet}$ implies a jet Lorentz factor of $\Gamma_{\rm jet} = 1.25$. Also, according to radio observations (Ray et al. 1997), the radio spectral index (α) can vary from -0.4 to 0 (where the flux density is $F_\nu \propto \nu^\alpha$), with $\alpha \sim -0.4$ in the quiescent state. These values of α, following the simple relationship $p = 1 - 2\alpha$ (only valid in the synchrotron optically thin regime), would imply a value of p in the range from 1 to 1.8, being the second number its value in the quiescent state. We will try values of p around its value in the quiescent state in our study. The observed spectrum above 100 MeV has been obtained from the third EGRET catalogue (Hartman et al. 1999). The total observed photon flux at energies higher than 100 MeV is about 8×10^{-7} photons cm^{-2} s^{-1}, and the observed photon index is $\Gamma = 2.2 \pm 0.1$ (photon flux per energy unit: $I_\epsilon \propto \epsilon^{-\Gamma}$). All these parameters have been summarized in Table 1.

To fix the γ-jet radius (R_γ), we have imposed that it should be at least of about few electron Larmor radii ($\sim 10^6$ cm), in order to keep those electrons confined inside the jet. Thus, R_γ has been taken to be 10^7 cm. To determine the power of the leptonic jet, we need to fix also the accretion luminosity of the disk (Falcke & Biermann 1996). A typical value for a microquasar with a high mass stellar companion can be $L_{\rm ac} \simeq 10^{-9}\ M_\odot\ c^2$ yr^{-1}. Both prior parameters can also be found in Table 1. $L_{\rm ke}$ will be fixed through comparison between the observed fluxes and the model. From the EGRET energy range, and the involved seed photon and electron energies in the scattering, the initial maximum Lorentz factor of the electrons should be about 10^4. Also, similar values for the maximum Lorentz factor were estimated from millimiter observations by Paredes et al. (2000b). A more accurate value for $\gamma_{\rm e0}^{\rm max}$ will be found when trying to reproduce the observed spectrum slope. Regarding B_γ, we will study our model behavior along a wide range of magnetic field values, from values of 1 G (close to the magnetic field strengths at the radio emitting zone, see Massi et al. 1993) to 100 G.

3.2. Results

We have computed the normalized spectral photon distributions for two different values of B_γ and $\gamma_{\rm e0}^{\rm max}$ (see Fig. 1). For $\gamma_{\rm e0}^{\rm max} = 10^4$ and $B_\gamma = 100$ G, the computed spectral photon index above 100 MeV is 2.4, which is steeper than the observed one (2.2 ± 0.1). In case that the magnetic field strength is lower, the spectrum will get softer. For $\gamma_{\rm e0}^{\rm max} = 10^5$ and $B_\gamma = 100$ G, the spectrum becomes more similar to the one observed in the EGRET energy range. Now, in case that the magnetic field strengh is lower the spectrum will get harder. About the electron power law index, we have found that a good value might be around 1.7, and higher values of p would imply a calculated photon index different from the one obtained from EGRET data (about 2 σ or more for p higher than 2). We want to remark

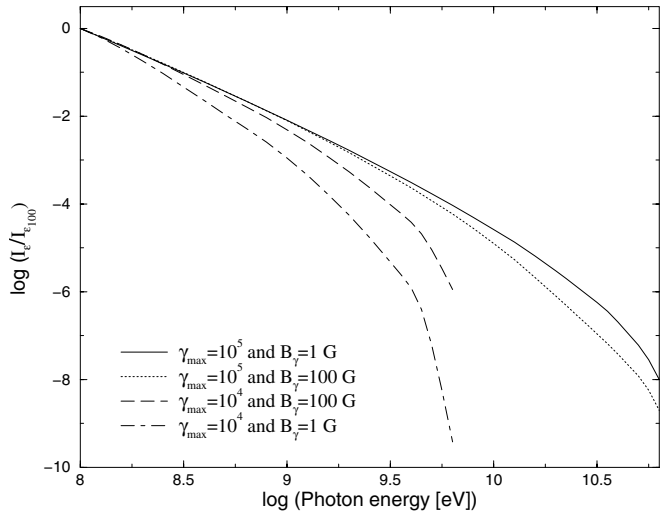

Fig. 1. Computed spectral photon distribution normalized to the photon flux value at 100 MeV for different values of the magnetic field and the maximum electron Lorentz factor. The solid and dotted lines represent $I'_{\epsilon'}$ for two different B_γ: 1 and 100 G, respectively, and a γ_{e0}^{max} of 10^5. The dot-dashed and dashed lines represent $I'_{\epsilon'}$ for two different B_γ: 1 and 100 G, respectively, and a γ_{e0}^{max} of 10^4.

Table 2. Two sets of free parameters used to reproduce the observations.

Parameter	dominant EC	dominant SSC
B_γ	1 G	10 G
L_{ke}	10^{35} erg/s	3×10^{35} erg/s
γ_{e0}^{max}	10^5	10^5

that p is the power-law of the initial electron energy distribution, and the spectral softening is a natural consequence of the introduction of losses in our model; it is not imposed a priori. Due to the lack of data beyond 10 GeV, we cannot still give a proper upper limit for γ_{e0}^{max}.

The values of the model parameters that reproduce properly the observations are shown in Table 2. We have taken separately the case in which the dominant source of seed photons is the companion star (i.e. $B_\gamma = 1$ G, see Figs. 2 and 3) and the case in which the dominant source of seed photons is the synchrotron process within the jet (i.e. $B_\gamma = 10$ G, see Fig. 4). Also, in order to study the implications on variability of the orbital eccentricity at the EGRET energy range, we have calculated the spectral photon distribution at an orbital distance equal to the orbital semi-major axis, at the periastron passage and at the apastron passage. However, in a first and simpler situation (Fig. 2), only the variations in the stellar photon density have been taken into account. In the other two cases (Figs. 3 and 4), accretion variation has been added. Following the accretion model of Bondi & Hoyle (1944), the accretion rate has been taken to be proportional to the density of the medium surrounding the compact object and further dependences have been neglected here. We have assumed also that the ambient density decreases like $1/R_{orb}^2$.

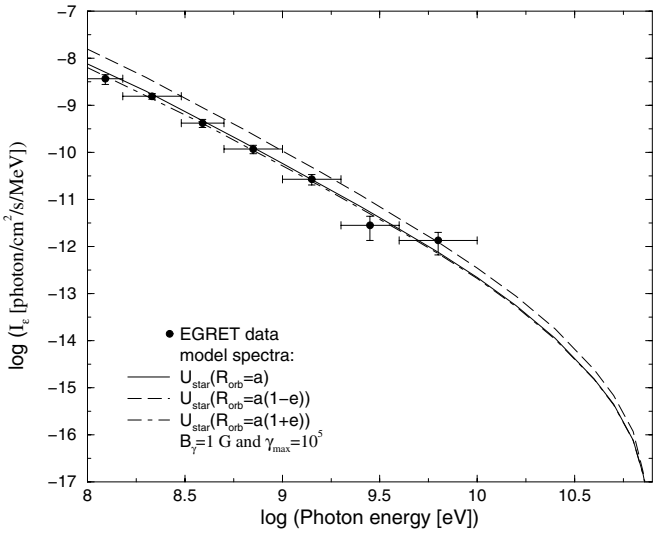

Fig. 2. Computed spectral photon distribution above 100 MeV plotted with the EGRET data points. Only changes in the stellar photon density have been taken into account and, due to the *low* magnetic field, EC dominates. p is taken to be 1.7, $\gamma_{e0}^{max} = 10^5$, and $B_\gamma = 1$ G. There are plotted the computed $I'_{\epsilon'}$ for different orbital radii: a (solid line), the distance at the periastron passage ($a(1-e)$, dashed line), and the distance at the apastron passage ($a(1+e)$, dotted line).

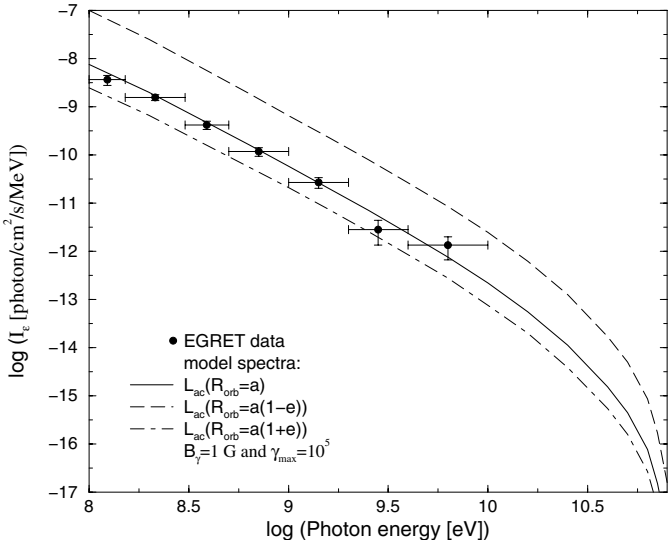

Fig. 3. Same as in Fig. 2 but now changes in both the stellar photon density and the accretion rate have been taken into account.

It is worth noting that, although for the two magnetic field strengths quoted before the spectral photon distribution is quite similar, the physical origin of the seed photons and the length of the γ-jet are different. When $B_\gamma = 1$ G, the length reached by the jet's electrons emitting at 100 MeV by IC process (the γ-jet length) is of about one astronomical unit whereas, for $B_\gamma = 10$ G, the length of such a jet is roughly one hundred times smaller.

4. Discussion

Our model is able to reproduce the observed data, supposing that the emission detected by EGRET comes from a compact

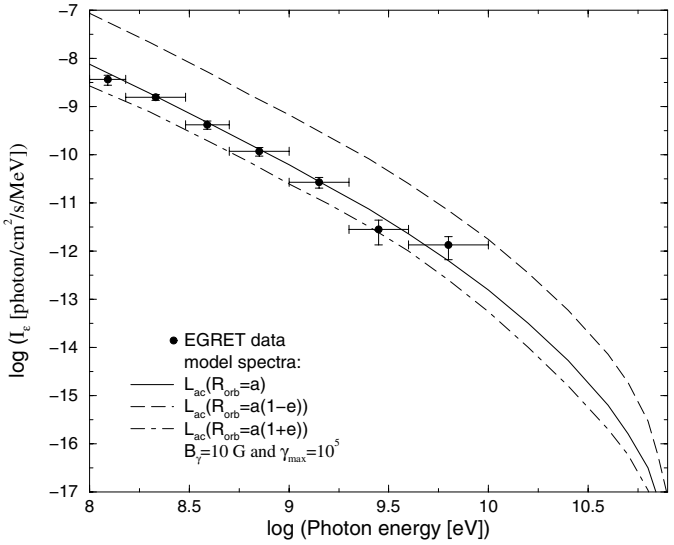

Fig. 4. Same as in Fig. 3 but with $B_\gamma = 10$ G.

cylindrical jet close to the compact object. In order to reach the observed levels of emission, a $L_{\rm ke}$ of 10^{35} erg/s for $B_\gamma = 1$ G, or of 3×10^{35} erg/s for $B_\gamma = 10$ G, is necessary. These values for the leptonic jet power are well within the limits given in the work of Falcke & Biermann (1996), using our adopted $L_{\rm ac}$. Regarding $\gamma_{\rm e0}^{\rm max}$, for a value of 10^5, the model reproduces properly the observations. Otherwise, future instruments covering EGRET and higher energy ranges (i.e. AGILE[3], GLAST[4], HESS[5], MAGIC[6]) will allow to get a better constraint on $\gamma_{\rm e0}^{\rm max}$, as well as will permit to check whether the predicted spectral shape follows the real source spectrum. Also, assuming that the electron energy distribution function is represented roughly by a power-law, we have found that p should be of about 1.7, which is also in agreement with radio observations in the quiescent state. This fact seems to suggest that both radiation types (radio and γ-rays) come from the jet. Our model also predicts that, during a flare, variations in both the intensity and the slope of the spectrum at higher energies should be detected in correlation with the ones observed at radio frequencies. This is not necessarily in contradiction with the observed shift in time of the emission peaks at different energy bands, which have been linked to changes in the environment and within the jet itself (Martí & Paredes 1995; Strickman et al. 1998; Gregory et al. 1999) and whose study is beyond the scope of this work. Otherwise, good timing and spectral resolution observations at high-energy γ-rays and coordinated observations at different energy bands are needed in order to find out whether both the low- and the high-energy emission have the same origin. We will not go, for the moment, into the study of the emission at frequencies below the high-energy γ-rays, being necessary to extend the modelisation of the jet up to bigger scales. A further comment can be done, regarding the role of the magnetic field in our model: unlike in some other developed models before, B_γ could play an important role in the generation of seed photons in the high energy IC emission. It is worth also mentioning that the upper limits of emission at hundreds of GeV (Hall et al. 2003) would be in agreement with the softening of the computed spectral photon distribution above ~10 GeV. This softening above ~10 GeV would make the source extremely faint at hundreds of GeV and above. The previous point and a spectrum at X-rays harder than at EGRET energies, likely due to the electron energy losses, seem to point to a dominant leptonic radiative mechanism in the jet (IC) instead to a hadronic one.

Regarding variability, our model predicts that important variations of the flux might occur along the eccentric orbit. For the sake of simplicity, we have contemplated two cases. The first one accounts for the variation of the EC photon flux along the orbit due only to the changes in the stellar photon density because of the eccentricity (see Fig. 2). This is only relevant if the SSC effect is not significant. The second one takes into account the variation of the IC photon fluxes due to the changes in both the stellar photon density and the accretion rate because of the orbital eccentricity (see Figs. 3 and 4). The high-energy γ-ray emission variability is clearly dominated by the accretion rate variations along the orbit. As it is mentioned in Sect. 1, the high-energy γ-ray emission of 3EG J0241+6103 varies a factor of 3. Also, all of the computed spectral photon distributions present fluxes that vary within a range of 2–30 times. Due to EGRET timing sensitivity, the periodic outburst at γ-rays associated to the periastron passage could not be sampled properly though the detected *averaged* emission could explain the observed variability of 3EG J0241+6103, and may be related to a radio outburst. Such a γ-ray outburst would be detected smoother and earlier in orbital phase than the radio one. If this is true, more sensitive timing observations at high-energy γ-rays along the orbit will find larger variability than the previously found. It is interesting to note that our model predicts a peak in the periastron at 0.2 (as it is found in the work of Massi 2004), when accretion rate is expected to be higher. The second peak at phase 0.5, mentioned in the Sect. 1, can be explained in the context of an eccentric orbit where the interaction between the compact object and the wind of the stellar companion produces an increase in the accretion rate under certain conditions (Martí & Paredes 1995). This would produce also a variability effect on the γ-ray flux like the one showed in Figs. 3 and 4.

Short timescale variability could be produced by precession (see, for instance, Kaufman Bernadó et al. 2002). In Massi et al. (2004), the authors found evidence of precession of the LSI +61°303's jets on timescales of a few days, similar to the shorter variability timescales found at high-energy γ-rays by Tavani et al. (1998) for 2CG 135+01. We have computed the fluxes for different values of the angle θ, from 0 to $\pi/2$, obtaining variations in the intensity of the IC emission of almost two orders of magnitud. This gives us just an upper limit for the intensity changes of the γ-ray emission due to precession, in agreement with observed variability at these energy ranges.

Regarding the effect of the magnetic field on the length-scale of the γ-jet, for B_γ above 10 G and due to the strong energy losses induced by the SSC effect, the electrons might need to be reaccelerated significantly after leaving the γ-jet

[3] http://agile.mi.iasf.cnr.it
[4] http://glast.gsfc.nasa.gov
[5] http://www.mpi-hd.mpg.de/hfm/HESS/HESS.html
[6] http://hegra1.mppmu.mpg.de/MAGICWeb/

to reach the observed radio jet. However, for B_γ lower than 10 G, reacceleration might not be necessary in regions closer to the compact object than the radio jet. It is remarkable that higher magnetic fields imply more seed photons though higher energy losses as well, and this is the reason why the leptonic jet power requirements are slightly different depending on the dominant mechanism of γ-ray emission, EC or SSC scattering (see Table 2).

Finally, comparing the results obtained applying our model to LSI +61°303 with the ones obtained in Bosch-Ramon & Paredes (2004) for LS 5039, we want to note the strong similarities shown by both sources. Nevertheless, it is remarkable that the jet power in the first case is ten times smaller than in the second one. This is related to the fact that both sources present different Lorentz factors. The Lorentz factor of the jet in LSI +61°303 is mildly relativistic but higher than the Lorentz factor of the jet in LS 5039 (1.25 and 1.02, respectively). This higher Lorentz factor has two effects. The first one is the increase of the observed flux due to the Doppler boosting, needing less kinetic power in the jet to explain the observed levels of emission. The second effect is an increase of the stellar seed photon density in the reference frame of the jet of LSI +61°303. This makes the photon field density of the stellar companion of LSI +61°303 (a B0 V star) in the reference frame of the jet to be similar to the one in the case of LS 5039 (a ON6.5 V((f)) star). Therefore, in order to know which source of seed photons can be dominant, is important also to have a good knowledge of both the jet kinematic characteristics and the angle between the jet and line of sight.

Acknowledgements. We are grateful to Marc Ribó and Gustavo E. Romero for their useful comments and suggestions. V.B.-R. and J.M.P. acknowledge partial support by DGI of the Ministerio de Ciencia y Tecnología (Spain) under grant AYA-2001-3092, as well as additional support from the European Regional Development Fund (ERDF/FEDER). During this work, V.B.-R. has been supported by the DGI of the Ministerio de Ciencia y Tecnología (Spain) under the fellowship FP-2001-2699. We thank an anonymous referee for constructive comments on the manuscript.

References

Apparao, K. M. V. 2001, A&A, 366, 865
Blumenthal, G. R., & Gould, R. J. 1970, RMP, 42, 237
Bondi, H., & Hoyle, F. 1944, MNRAS, 104, 273
Bosch-Ramon, V., & Paredes, J. M. 2004, A&A, 417, 1075
Bosch-Ramon, V., Romero, G. E., & Paredes, J. M. 2004, A&A, submitted
Casares, J., Ribas, I., Paredes, J. M., & Martí, J. 2004, A&A, submitted
Dermer, C. D., & Schlickeiser, R. 2002, ApJ, 575, 667
Falcke, H., & Biermann, P. L. 1996, A&A, 308, 321
Frail, D. A., & Hjellming, R. M. 1991, AJ, 101, 2126
Goldoni, P., & Mereghetti, S. 1995, A&A, 299, 751
Gregory, P. C. 2002, ApJ, 575, 427
Gregory, P. C., & Taylor, A. R. 1978, Nature, 272, 704
Gregory, P. C., Xu, H., Backhouse, C. J., & Reid, A. 1989, ApJ, 339, 1054
Gregory, P. C., Peracaula, M., & Taylor, A. R. 1999, ApJ, 520, 376
Hall, T. A., Bond, I. H., Bradbury, S .M., et al. 2003, ApJ, 583, 853
Harrison, F. A., Ray, P. S., Leahy, D. A., Waltman, E. B., & Pooley, G. G. 2000, ApJ, 528, 454
Hartman, R. C., Bertsch, D. L., & Bloom, S. D., et al. 1999, ApJS, 123, 79
Hermsen, W., Swanenburg, B. N., Bignami, G. F., et al. 1977, Nature, 269, 494
Hutchings, J. B., & Crampton, D. 1981, PASP, 93, 486
Kaufman Bernadó, M. M., Romero, G. E., & Mirabel, I. F. 2002, A&A, 385, L10
Kniffen, D. A., Alberts, W. C. K., Bertsch, D. L., et al. 1997, ApJ, 486, 126
Leahy, D. A. 2001, A&A, 380, 516
Leahy, D. A. 2004, A&A, 413, 1019
Maraschi, L., & Treves, A. 1981, MNRAS, 194, 1P
Martí, J., & Paredes, J. M. 1995, A&A, 298, 151
Massi, M. 2004, A&A, 422, 267
Massi, M., Paredes, J. M., Estalella, R., & Felli, M. 1993, A&A, 269, 249
Massi, M., Ribó, M., Paredes, J. M., Peracaula, M., & Estalella, R. 2001, A&A, 376, 217
Massi, M., Ribó, M., Paredes, J. M., et al. 2004, A&A, 414, L1
McSwain, M. V., Gies, D. R., Huang, W., et al. 2004, ApJ, 600, 927
Mirabel, I. F., & Rodríguez, L. F. 1999, ARA&A, 37, 409
Paredes, J. M. 1987, Ph.D. Thesis, Universitat de Barcelona
Paredes, J. M., & Figueras, F. 1986, A&A, 154, L30
Paredes, J. M., Martí, J., Ribó, M., & Massi, M. 2000a, Science, 288, 2340
Paredes, J. M., Martí, J., Peracaula, M., Pooley, G., & Mirabel, I. F. 2000b, A&A, 357, 507
Peracaula, M. 1997, Ph.D. Thesis, Universitat de barcelona
Punsly, B. 1999, ApJ, 519, 336
Ray, P. S., Foster, R. S., Waltman, E. B., Tavani, M., & Ghigo, F. D. 1997, ApJ, 491, 381
Ribó, M. 2002, Ph.D. Thesis, Universitat de Barcelona
Romero, G. E., Torres, D. F., Kaufman Bernadó, M. M., & Mirabel, I. F. 2003, A&A, 410, L1
Strickman, M. S., Tavani, M., Coe, M. J., et al. 1998, ApJ, 497, 419
Swanenburg, B. N., Bennett, K., Bignami, G. F., et al. 1981, ApJ, 243, L69
Tavani, M., Kniffen, D., Mattox, J. R., Paredes, J. M., & Foster, R. 1998, ApJ, 497, L89
Taylor, A. R., & Gregory, P. C. 1982, ApJ, 255, 210
Taylor, A. R., Gregory, P. C., Hutchings, J. B., & Crampton, D. 1980, IAU Circ., 3464, 3
Taylor, A. R., Young, G., Peracaula, M., Kenny, H. T., & Gregory, P. C. 1996, A&A, 305, 817
Wallace, P. M., Griffis, N. J., Bertsch, D. L., et al. 2000, ApJ, 540, 184